ELSEVIER

Journal of Molecular Catalysis A: Chemical 115 (1997) 421–429

JOURNAL OF MOLECULAR CATALYSIS A: CHEMICAL

Surface electronic structure and reactivity of transition and noble metals [1]

A. Ruban *, B. Hammer, P. Stoltze, H.L. Skriver, J.K. Nørskov

CAMP, Department of Physics, Technical University of Denmark, DK-2800 Lyngby, Denmark

Abstract

We present self-consistent density functional calculations using the LMTO-ASA method of the variations in the surface electronic structure for pseudomorfic overlayers and impurities of Fe, Co, Ni, Cu, Ru, Rh, Pd, Ag, Ir, Pt, and Au on the other metals. Knowledge of these variations is of importance in understanding trends in the reactivity of metal surfaces. A simple model is presented which gives a description of the overall trends in the self-consistently calculated results.

1. Introduction

It is one of the long term goals of surface science to provide an understanding of the properties of metal surfaces that determine their reactivity. If such an understanding can be established, it would be possible to predict the reactivity of a given surface, including the effect of structure, the effect of alloying and the effect of co-adsorbed species. This would open very interesting possibilities in the *design* of surfaces with specific catalytic properties.

We are still far from such an understanding, but new possibilities have emerged recently due to the developments in density functional theory. By a combination of new numerical techniques (for a review, see [1]), a better, non-local description of exchange and correlation effects [2,3], and faster computers it is now possible to describe the energetics of adsorption and dissociation reactions with an accuracy of the order 0.2 eV [3–17]. While this is not a sufficient accuracy for the calculation of chemical rates, it is reasonable for studying trends. Using the density functional calculations as *computer experiments* we can study systematically which surface parameters influence the reactivity. In the computer experiments we are free to study the role of electronic and geometric effects separately. When comparing the barrier for dissociation for e.g. H_2 on Cu(111) and (100), the barrier height can first be compared for like reaction geometries, and later the effect of the different possible reaction paths on the two surfaces can be compared [18]. Similarly, one can single out the role of surface relaxation by first considering the unrelaxed surface and afterwards include the motion of the substrate during the reaction.

Studies so far of a limited number of adsorbates and surfaces [15–17,19] have led to the formulation of a simple model of surface reac-

* Corresponding author.

[1] Communication presented at the First Francqui Colloquium, Brussels, 19–20 February 1996.

PII S1381-1169(96)00348-2

tivity of transition and noble metals. The model singles out three surface properties contributing to the ability of the surface to make and break adsorbate bonds: (i) the center ϵ_d of the d-bands, (ii) the degree of filling f_d of the d-bands, and (iii) the coupling matrix element V_{ad} between the adsorbate states and the metal d-states. The basic idea is that *trends* in the interaction energy between an adsorbate and a metal surface are governed by the coupling to the metal d-bands, since the coupling to the metal sp states is essentially the same for the transition and noble metals. The coupling between the adsorbate and the surface is therefore included in two steps. First, the adsorbate is coupled to the metal sp states. This leads to a shift and broadening of the adsorbate states, and to a substantial part of the adsorption energy. The renormalized adsorbate states are then coupled to the metal d-states. If the inclusion of the coupling to the d-states is a small perturbation of the system then this contribution to the total energy can be calculated simply from the change of the sum of the (Kohn–Sham) one-electron energies. This follows from the frozen potential approximation [20] or the force theorem [21]. If the coupling to the metal sp states can be considered to be similar for a group of surfaces, trends in adsorption energies will depend primarily on the coupling to the metal d-states, which then depends primarily on the three factors listed above. Other factors like the width and shape of the d-band also influence the coupling energy, but these are generally smaller corrections [22].

If the coupling is weak ($|V_{ad}| \ll |\epsilon_d - \epsilon_a|$) the interaction between an adsorbate state with filling f_a at energy ϵ_a and a metal d-state with filling f_d at ϵ_d can be written

$$E_{d-hyb} = -C(f_a, f_d)\frac{V_{ad}^2}{|\epsilon_a - \epsilon_d|} + \alpha V_{ad}^2 \qquad (1)$$

where $C(f_a, f_d)$ only depends on the number of electrons in the adsorbate state and the metal d-bands. The first term is the hybridization energy leading to an attraction if the anti-bonding states are not completely filled, while the second term gives the repulsion due to the orthogonalization between the adsorbate and metal d-states. Clearly, the center of the d-band ϵ_d is an important parameter characterizing the ability of the surface d-electrons to participate in bonding to the adsorbate. The d-band center of a given metal atom will depend on the surroundings, and one of the possibilities for modifying the reactivity of a metal is by depositing it as an overlayer [23] or alloy it into the surface layer of another metal [24]. Alloying is extensively used to modify the activity of high surface area systems [25,26].

For a given adsorbate, f_a is fixed, and the other two parameters determining the interaction energy with the d-states are (i) the filling of the d-bands, f_d, and (ii) the coupling matrix element V_{ad}.

Let us consider CO adsorption on a metal surface as an example. There are two valence states of the CO that couple strongly to the metal d-states, the filled 5σ and the empty $2\pi^*$ states [27–29]. For each of these states we can estimate the interaction with the d-bands based on Eq. (1). In Fig. 1 we compare the result of such an analysis to self-consistently calculated CO chemisorption energies [17]. There is clearly a very good correlation between the calculated adsorption energies (which also agree very well with experimentally determined values [17]) and the model.

One of the important results of Fig. 1 is that the variations in the CO bond energy when one metal is deposited on another are well described. CO adsorbs much stronger on a monolayer of Cu on Pt(111) than on the clean Cu(111) surface for instance. The same is true for Ni on Ru(0001) while the opposite holds for Pd on Ru(0001). This is also observed experimentally [23]. The variations can be traced simply to the variations in the d-band centers. For CO adsorption on the late transition metals the coupling of the $2\pi^*$ level to the d-bands is much stronger than the coupling of the 5σ level [17]. The

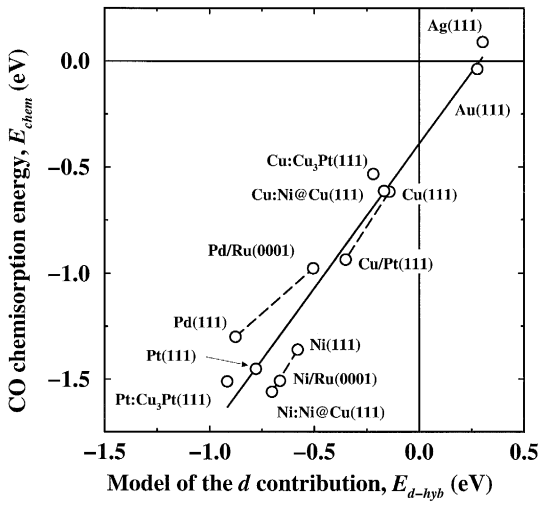

Fig. 1. The chemisorption energy, E_{chem}, of CO at various metal and bimetal surfaces as calculated in density functional theory versus the simple model estimate, $E_{\mathrm{d-hyb}}$ (Eq. (1)) of the hybridization energy between the CO $2\pi^*$ and 5σ and the metal d states at the surface [17]. $M_1/M_2(111)$ refers to CO chemisorption at a pseudomorphic monolayer of M_1 over a $M_2(111)$ substrate, M_1:M_1@$M_2(111)$ to CO chemisorption at the M_1 site of a $1/4$ monolayer of M_1 'impurity' atoms substituted into a $M_2(111)$ surface, etc. As indicated by the solid line, the overall trends in E_{chem} are contained in the simple $E_{\mathrm{d-hyb}}$ expression. The dashed lines further emphasize that in particular the trends in the chemisorption energy of CO at one metal species in different metallic environments are captured by $E_{\mathrm{d-hyb}}$.

change in the chemisorption energy due to a change in the d-band center by $\delta\epsilon_{\mathrm{d}}$ is therefore

$$\delta E_{\mathrm{d-hyb}} \sim 4 f_{\mathrm{d}} \frac{V_{2\pi-\mathrm{d}}^2}{\left(\epsilon_{2\pi}-\epsilon_{\mathrm{d}}\right)^2}\delta\epsilon_{\mathrm{d}} \equiv \gamma\delta\epsilon_{\mathrm{d}} \qquad (2)$$

This means that $\delta E_{\mathrm{d-hyb}}/\gamma$ and therefore $\delta E_{\mathrm{chem}}/\gamma$ should be proportional to the change in the d-band center $\delta\epsilon_{\mathrm{d}}$. This is illustrated in Fig. 2 for the three cases discussed above. The self-consistently calculated change in the CO chemisorption energy is clearly given by $\delta\epsilon_{\mathrm{d}}$ as predicted by the model. Since the $2\pi^*$ level is above the Fermi level the interaction with the d-band becomes stronger when the d-band shifts up as is the case for Cu/Pt(111) so that the energy denominator in Eq. (1) becomes smaller. When Ni is deposited as a monolayer on Ru or as an impurity in Cu(111) the d-bands also shift up while the opposite is true for Pd when deposited on Ru(0001).

A similar picture is expected to hold for other molecular adsorbates with empty or partly empty states above the Fermi level (N_2, NO, O_2, CH_4, other hydrocarbons, etc). Clearly, the variations in the center of the d-bands is an important (but not necessarily the only) parameter in understanding variations in adsorption energies and activation energies from one metal to the next.

In the present paper we present density functional calculations of the change in ϵ_{d} when a number of metals form overlayers or are alloyed into the first layer of other metals. We study all the combinations of metals to the right of and including the Fe group, since these systems contain a number of the metal combinations that could be of interest in catalysis.

The main results of this study have been obtained by fully self-consistent calculations of d-band centers using the linear muffin–tin or-

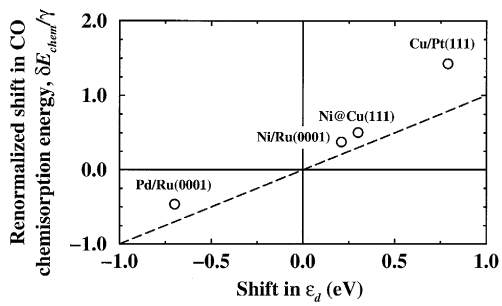

Fig. 2. The density functional theory based chemisorption energy shifts from CO adsorption at the Ni, Cu or Pd(111) surfaces to adsorption at impurity or overlayer structures plotted versus the shifts in the valence d centers at the involved surface metal atom (before the CO adsorption). The chemisorption energy shifts are renormalized with γ (defined in Eq. (2)) so that the different coupling strengths of Ni, Cu and Pd to CO have been taken into account. The dashed line shows the renormalized gain in $2\pi^*$–metal d hybridization energy (to first order in the ϵ_{d} shift) which is the dominant part of $E_{\mathrm{d-hyb}}$. As ϵ_{d} shifts up in energy (closer to $\epsilon_{2\pi}$) the CO–metal bond strength increases in both the full calculation and in the model. Likewise, a downshift of ϵ_{d} gives a weaker CO–metal bond. Note that in Ref. [17] γ is calculated relative to the value for Cu(111), while here the absolute values are used. Also note that the shifts in ϵ_{d} are taken from Ref. [17] where they are calculated in a plane wave pseudopotential approach and that they therefore differ slightly from the LMTO-ASA based numbers in Table 1.

bitals (LMTO) method within the atomic sphere approximation (ASA) [21]. This method has allowed us to study the trends for a whole set of systems, but only for a pseudomorphic, unrelaxed overlayer and surface impurities at the ideal substrate lattice positions. We first present these results. We then develop a simple model which is able to describe the overall trends seen in the full calculation. Finally, we also discuss trends in the other surface parameters determining the reactivity.

2. Calculational method

All the results presented in this section are based on density functional calculations within the local density approximation. We have been using the LMTO-ASA method to solve the Kohn–Sham equations. The method is computationally very efficient, and this has allowed us to calculate trends for 110 combinations of metals. The disadvantage of the method is that lattice relaxations are not easily included.

In the LMTO-ASA calculations we applied the Green function technique in conjunction with the coherent potential approximation (CPA) for alloy surfaces [30,31]. Six layers of atomic spheres and two layers of the vacuum spheres have been treated self-consistently with the equilibrium lattice spacing of a substrate obtained in the bulk self-consistent LMTO-ASA calculations. For the impurities we considered the dilute limit of a completely random surface alloy with the concentration one at% of a solute. To take into account the charge transfer effects in the single-site approximation in this case the screened impurity model has been used in the definition of the Madelung potential [32,33]. All the calculations have been spin-restricted with the Perdew–Zunger parameterization [34] of the results of Ceperley and Alder [35] for exchange and correlation.

We always consider the most close packed surface ((111) for fcc, (0001) for hcp and (110) for bcc).

3. Calculated variations in d-band centers for unrelaxed, pseudomorphic overlayers and surface impurities

Table 1 summarizes the results for the d-band centers, ϵ_d, defined as the centroid of the d-type density of states in an atomic sphere centered at a surface atom. This quantity is often referred to as C_d in the LMTO literature. Along the diagonal are shown the calculated d-band centers of the most close packed surface of the elemental metals and the off-diagonal elements show the shift in the d-band center when one metal is alloyed into the surface layer or form a pseudomorphic overlayer on one of the other metals. For each metal we have considered the equilibrium bulk metal structure (fcc, hcp or bcc) for the substrate, but we have found that variations of d-band centers for the close-packed surfaces of the different structures are small, of order 0.02–0.04 eV in the case of fcc(111) and bcc(110) and even smaller in the case of hcp(0001) and fcc(111) faces. The differences between different facets of the same bulk structure are generally larger, of order 0.2 eV in the case of fcc(111) and fcc(100) facets.

We point out again, that the results are for overlayers and surface impurities occupying lattice positions of the substrate, and we have not here taken into account whether these structures are actually stable under experimental conditions. Yet, the table can be used to get an idea about possible ways of modifying the electronic structure of a surface. As we will show later, there is a tendency that the inclusion of relaxations will decrease the shifts seen in Table 1, but this will not in general change the sign or relative magnitude of the effect.

It is seen that there is a tendency that when the early (small) elements in the table are alloyed into or put on top of the later (larger) elements, the d-band center shifts up. According to the arguments above this should lead to an increase in the interaction with molecules like CO. Likewise, we see that a large atom on top of a metal with a smaller Wigner–Seitz radius

tends to give rise to a down-shift of the d-states and thus to a decrease of the CO bonding (an increase in the energy of the system).

4. A simple model for the overall trends in the d-band shifts

To understand the origin of the main trends in Table 1 we build on the observation above that the sign and magnitude of the shifts seem to depend on the difference in the size of the two metals. It is well known from LMTO theory that the d-band centers ϵ_d depend sensitively on the Wigner–Seitz radius s. In fact, $d\epsilon_d/d\ln s$ have been tabulated for all the elemental metals [21]. Values of s and $d\epsilon_d/d\ln s$ for all 3d, 4d, and 5d transition and noble metals are given in Fig. 3. The concept of a Wigner–Seitz radius containing a neutral atom in a perfect solid can be generalized by the neutral radius, defined to contain a neutral atom for any configuration. For a surface atom the neutral radius is larger than in the bulk because the contribution to the electron density around a surface atom from the neighbors is smaller than in the bulk. It is seen in Fig. 3 that $d\epsilon_d/d\ln s$ is positive for all the metals to be considered here (Fe–Cu, Ru–Ag, Ir–Au). Consequently the d-band centers at the surface are higher in energy than for the bulk. This is in accordance with experience from the self-consistent density functional calculations.

We now follow the effective medium theory (EMT) [20,36] and approximate the electron density in the system by a superposition of atom-like electron densities at each atom. In this case, there is a one to one relation between the neutral radius s_i for an atom i in the system and the average electron density $\bar{n}_i$ from the neighbors around atom i. Based on density functional calculations for atoms embedded in

Table 1
Shifts in d-band centers of surface impurities and overlayers relative to the clean metal values (italic)

	Fe	Co	Ni	Cu	Ru	Rh	Pd	Ag	Ir	Pt	Au
Fe	*−0.92*	0.05	−0.20	−0.13	−0.29	−0.54	−1.24	−0.83	−0.36	−1.09	−1.42
		0.14	−0.04	−0.05	−0.73	−0.72	−1.32	−1.25	−0.95	−1.48	−2.19
Co	0.01	*−1.17*	−0.28	−0.16	−0.24	−0.58	−1.37	−0.91	−0.36	−1.19	−1.56
	−0.01		−0.20	−0.06	−0.70	−0.95	−1.65	−1.36	−1.09	−1.89	−2.39
Ni	0.09	0.19	*−1.29*	0.19	−0.14	−0.31	−0.97	−0.53	−0.14	−0.80	−1.13
	0.96	0.11		0.12	−0.63	−0.74	−1.32	−1.14	−0.86	−1.53	−2.10
Cu	0.56	0.60	0.27	*−2.67*	0.58	0.32	−0.64	−0.70	0.58	−0.33	−1.09
	0.25	0.38	0.18		−0.22	−0.27	−1.04	−1.21	−0.32	−1.15	−1.96
Ru	0.21	0.26	0.01	0.12	*−1.41*	−0.17	−0.82	−0.27	0.02	−0.62	−0.84
	0.30	0.37	0.29	0.30		−0.12	−0.47	−0.40	−0.13	−0.61	−0.86
Rh	0.24	0.34	0.16	0.44	0.04	*−1.73*	−0.54	0.07	0.17	−0.35	−0.49
	0.31	0.41	0.34	0.22	0.03		−0.39	−0.08	0.03	−0.45	−0.57
Pd	0.37	0.54	0.50	0.94	0.24	0.36	*−1.83*	0.59	0.53	0.19	0.17
	0.36	0.54	0.54	0.80	−0.11	0.25		0.15	0.31	0.04	−0.14
Ag	0.72	0.84	0.67	0.47	0.84	0.86	0.14	*−4.30*	1.14	0.50	−0.15
	0.55	0.74	0.68	0.62	0.50	0.67	0.27		0.80	0.37	−0.21
Ir	0.21	0.27	0.05	0.21	0.09	−0.15	−0.73	−0.13	*−2.11*	−0.56	−0.74
	0.33	0.40	0.33	0.56	−0.01	−0.03	−0.42	−0.09		−0.49	−0.59
Pt	0.33	0.48	0.40	0.72	0.14	0.23	−0.17	0.44	0.38	*−2.25*	−0.05
	0.35	0.53	0.54	0.78	0.12	0.24	0.02	0.19	0.29		−0.08
Au	0.63	0.77	0.63	0.55	0.70	0.75	0.17	0.21	0.98	0.46	*−3.56*
	0.53	0.74	0.71	0.70	0.47	0.67	0.35	0.12	0.79	0.43	

The impurity/overlayer atoms are listed horizontally and the host entries are listed vertically. For each combination of the two numbers listed is first the isolated surface impurity given and than the overlayer. The surfaces considered are the most close packed and the overlayer structures are pseudomorphic. No relaxations from the host lattice positions are included. All values are in eV and the elemental d band centers are relative to the Fermi level.

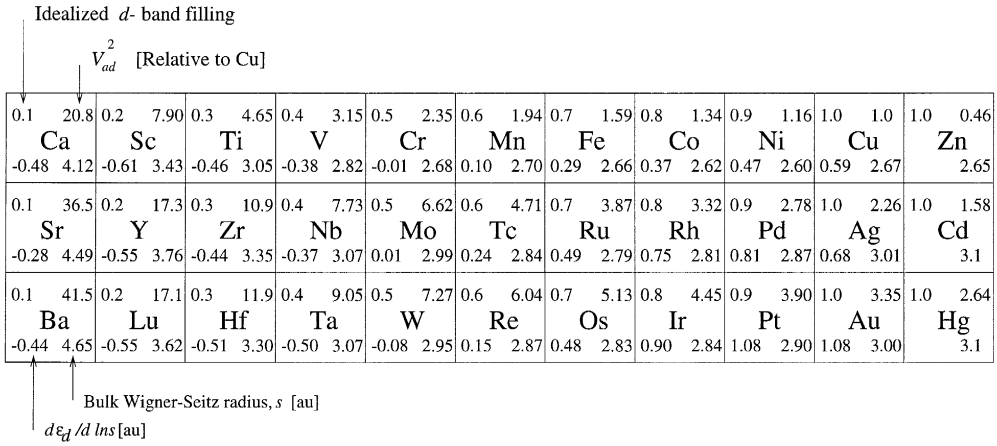

Fig. 3. Section of the periodic table with the 3d, 4d, and 5d transition metals and the noble metals. Shown in lower right corner: bulk Wigner–Seitz radius, s. Lower left corner: the $\mathrm{d}\epsilon_\mathrm{d}/\mathrm{d}\ln s$ which is used in Eq. (5). Note how this changes its sign through a row at about half d band filling as expected from the rigid band model. In the upper right corner: behavior of the adsorbate (s or p)–metal d coupling matrix element squared, V_{ad}^2. The V_{ad}^2's generally decrease for increasing nuclear charge within a row and increase down the groups. (This behavior of the coupling matrix elements is explored in [15] in the discussion of the origin of the nobleness of gold. Note that the coupling matrix elements of Co and Ni are misprinted in Fig. 4 of Ref. [15] — without, however, changing the ordering of the coupling matrix elements and therefore without affecting the reasoning in Ref. [15].) All above numbers except for the properties of Zn, Cd, and Hg, have been compiled from Ref. [21]. Finally, upper left corner: the idealized d band fillings. These are found to be close to the actual, calculated bulk d band fillings considering the uncertainties in interpreting these [21].

jellium, this relation has been found to be exponential [20]:

$$\bar{n}_i = n_0 \mathrm{e}^{-\eta(s_i - s_0)} \tag{3}$$

We now characterize the atom in which we are interested in the d-band center by its average electron density $\bar{n}_i$ and write

$$\delta\epsilon_\mathrm{d} = \frac{\mathrm{d}\epsilon_\mathrm{d}}{\mathrm{d}\ln s}\frac{\mathrm{d}\ln s}{\mathrm{d}\bar{n}}\delta\bar{n} \tag{4}$$

$$= -\frac{1}{\eta s_0}\frac{\mathrm{d}\epsilon_d}{\mathrm{d}\ln s}\frac{\delta\bar{n}}{n_0}. \tag{5}$$

For the six metals Ni, Pd, Pt, Cu, Ag, and Au we have EMT-parameters [36] and we can calculate the difference $\delta\bar{n}$ between $\bar{n}$ for an atom in the unrelaxed overlayer on top the (111) surface of any of the other metals and in the (111) surface of the elemental metal itself. Using the values of $\mathrm{d}\epsilon_\mathrm{d}/\mathrm{d}\ln s$ from Fig. 3 we get an estimate for the shifts in the d-band centers $\delta\epsilon_\mathrm{d}$ from Eq. (5). These results are compared to the self-consistently calculated results from Table 1 in Fig. 4. It can be seen that the overall trends are well described by the simple model, while the finer details are not. This confirms that an important effect of moving a layer of one kind of metal atoms to another substrate is to change the electron density or the 'size' of the atom. This in turn changes the center of the d-bands.

In addition, there will of course be changes in the d-band centers for overlayers due to hybridization between the overlayer/impurity d-states and the substrate d-states. Such effects

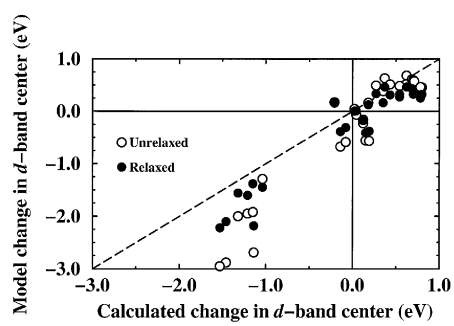

Fig. 4. Open circles: correlation between the LMTO-ASA based d band centers and the simple model estimate based on volume effects as described by Eq. (5) for unrelaxed impurity or overlayer systems of Ni, Pd, Pt, Cu, Ag, and Au. Solid circles: Effect of the relaxation as found by the model estimate.

may well account for the variations that are not accounted for by the simple model.

The change of the d-band center with the surrounding density is very simple to understand. As the environment of a surface metal atom changes, its embedding density, $\bar{n}$, changes and so does the local bandwidth of the d-bands. Given that metal impurity or overlayer systems of the type considered here strongly disfavor a net change in the local occupation of d-states at any site (i.e. the Hubbard U is large), the center of the d-bands will move in response to the changed d-band width. This, rigid band type model is schematically illustrated in Fig. 5. For the metals considered here, where the d-bands are more than half filled, a decreased embedding density and the accompanying d-band narrowing will give rise to an upshift of ϵ_d (as $d\epsilon_d/d\ln s > 0$ see Fig. 3). For transition metals to the left in the series where the d-bands are less than half filled a downshift of ϵ_d would result in order to maintain the same d-band filling (as $d\epsilon_d/d\ln s > 0$). For the noble metals the d-bands are fully occupied and are as such free to move in energy with changing the occupation. However, also for these systems the d-band positions will correlate with the embedding density as this determines the average potential (and hence the d-band position) through its contribution to the exchange–correlation potential.

We notice that the same arguments should hold for the core levels. They will shift with the embedding density in just the same way as the valence d-states through the shift in the entire local potential at the surface sites. The present arguments could therefore also be used to understand the overall trends in surface core level shifts. A similar picture has been derived from a completely different starting point by Ganduglia-Pirovano et al. [37].

We can use the effective medium based model above to estimate part of the effect of relaxations for the six metals where we have EMT parameters. The part that we can include is the effect of the change in density (or potential)

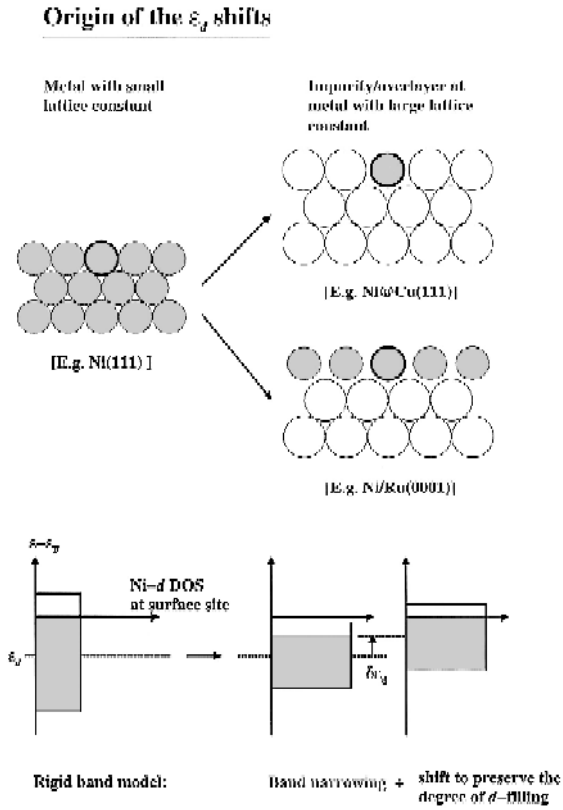

Fig. 5. When a metal atom (small grey circle) with a small lattice constant (and $f_d > 0.5$) is put as an impurity or overlayer at the surface of a metal (large white circles) with a large lattice constant, the embedding density and therefore the local d-band width are lowered and the center of the d band is caused to shift up in order to preserve the degree of d-band filling (grey shaded area). For a large metal atom on a small metal atom substrate the opposite is found.

from the neighbors. The shifts due to hybridization are not included. To get the potential shift, we simply let the overlayers relax in the EMT and recalculate $\delta\bar{n}$ and the model value for $\delta\epsilon_d$. This is also included in Fig. 4. It can be seen that the effect of the potential shift is quite small. It generally reduces $\delta\epsilon_d$ (the surface atoms move closer to the substrate, the density increases and the d-band width goes up), but it never changes the sign.

5. Trends in matrix elements

For completeness we also discuss how variations in the coupling matrix elements V_{ad} from

one metal to the next can be estimated from LMTO theory. As shown in Refs. [20,21,38] the coupling matrix element between an adsorbate state and a metal d-state a distance r away can be written

$$V_{ad} = \eta \frac{M_a M_d}{r^{l_a + l_d + 1}} \quad (6)$$

where η is given by the structure constants in LMTO theory and l_a denotes the angular momentum quantum number of the adsorbate state and l_d of the metal d-state. M_a and M_d are related to the LMTO potential parameters Δ by

$$M_l = \left(s^{2l+1} \Delta_l \right)^{1/2} \quad (7)$$

Here s denotes the neutral sphere radius for the atom in question. It is seen that for a given adsorbate at a given distance from a metal atom, the trends in the matrix element for the metals will depend only on M_d. Since the values for Δ for the bulk metals have been tabulated for all the metals [21] we can also tabulate the relative values of the matrix elements. In Fig. 3 we present $V_{ad}^2 \propto M_d^2$ relative to the value for Cu for the relevant section of the periodic table. We have used the bulk Wigner–Seitz radii as well as the bulk metal values for Δ in calculating M_d. Direct calculations show that this is a good approximation even for the surface.

In Fig. 3 we also include values for the filling of the d-bands. A filling factor $f_d = 0.8$ means that the d-bands have $0.8 \times 10 = 8$ electrons. The occupancy of the d-bands has been rounded off to correspond to an integer number of electrons for each metal. For the overlayers we find that the occupancies always remain equal to the elemental metal values on this scale.

6. Summary

In the present paper we have presented the results of a density functional calculation of several parameters describing the electronic structure of the metal surfaces and in particular surface alloys and overlayers. The major part of the paper has concentrated on the center of the d-bands. The d-band center is expected to be an important parameter determining the ability of the surface to bond to several adsorbates. Focusing of the metals Fe, Co, Ni, Cu, Ru, Rh, Pd, Ag, Ir, Pt, and Au we have calculated the d-band centers for the most close-packed surfaces of the elemental metals. For all combinations of the metals we have calculated the shift in the d-band center when the metal is alloyed into the surface of the other or is deposited as a pseudomorphic overlayer. These calculations have been for all atoms at the substrate lattice positions. These results can therefore only be taken as guidelines, the question whether such a structure can actually be formed in reality is not taken into account.

We have also developed a simple model to explain the overall trends the shifts in the d-band positions due to surface alloying or overlayer formation. The main variations can be well accounted for considering the changes in the electron density from the neighbors and the local d-band width. If a ‘small’ metal atom is moved into the lattice of a ‘larger’ one, the neighbors are further away and the d-band width at the atom becomes smaller than at the surface of the elemental metal. This brings about an up-shift in the d-band center in order to maintain the same d-band filling locally. Based on the model we also discuss the effect of lattice relaxations and reconstructions.

Finally, we have also discussed the variations in the coupling matrix elements between an adsorbate and the d-states of a metal surface and the filling of the d-bands in the relevant part of the periodic table.

Acknowledgements

The present work was in part financed by The Danish Research Councils through The Center for Surface Reactivity and grant #9501775. Center for Atomic-Scale Materials

Physics (CAMP) is sponsored by the Danish National Research Foundation.

References

[1] M.C. Payne, M.P. Teter, D.C. Allan, T.A. Arias and J.D. Joannopoulos, Rev. Mod. Phys. 64 (1992) 1045.
[2] J.P. Perdew, J.A. Chevary, S.H. Vosko, K.A. Jackson, M.R. Pederson, D.J. Singh and C. Fiolhais, Phys. Rev. B 46 (1992) 6671.
[3] B. Hammer, K.W. Jacobsen and J.K. Nørskov, Phys. Rev. Lett. 70 (1993) 3971; K. Gundersen, K.W. Jacobsen, J.K. Nørskov and B. Hammer, Surf. Sci. 304 (1994) 131.
[4] B. Hammer, M. Scheffler, K.W. Jacobsen and J.K. Nørskov, Phys. Rev. Lett. 73 (1994) 1400.
[5] J.A. White, D.M. Bird, M.C. Payne and I. Stich, Phys. Rev. Lett. 73 (1994) 1404.
[6] P.H.T. Philipsen, G. te Velde and E.J. Baerends, Chem. Phys. Lett. 226 (1994) 583.
[7] P. Hu, D.A. King, S. Crampin, M.-H. Lee and M.C. Payne, Chem. Phys. Lett. 230 (1994) 501.
[8] R.A. van Santen and M. Neurock, Catal. Rev., in print.
[9] H. Burghgraef, A.P.J. Jansen and R.A. van Santen, J. Chem. Phys. 101 (1994) 11012.
[10] H. Yang and J.L. Whitten, J. Chem. Phys. 96 (1992) 5529.
[11] O. Swang, J.K. Faegri, O. Gropen, U. Wahlgren and P.E.M. Siegbahn, Chem. Phys. 156 (1991) 379.
[12] B. Hammer and M. Scheffler, Phys. Rev. Lett. 74 (1995) 3487.
[13] J.A. White, D.M. Bird and M.C. Payne, Phys. Rev. B 53 (1996) 1667.
[14] S. Wilke and M. Scheffler, Phys. Rev. B 53 (1996) 4926.
[15] B. Hammer and J.K. Nørskov, Nature 376 (1995) 238.
[16] B. Hammer and J.K. Nørskov, Surf. Sci. 343 (1995) 211.
[17] B. Hammer, Y. Morikawa and J.K. Nørskov, Phys. Rev. Lett. 76 (1996) 2141.
[18] P. Kratzer, B. Hammer and J.K. Nørskov, Surf. Sci., in print.
[19] B.I. Lundqvist, O. Gunnarsson, H. Hjelmberg and J.K. Nørskov, Surf. Sci. 89 (1979) 196; S. Holloway, B.I. Lundqvist and J.K. Nørskov, Proc. Int. Congress on Catalysis, Berlin 1984, Vol. 4, p. 85–95; J.K. Nørskov, Rep. Prog. Phys. 53 (1990) 1253.
[20] K.W. Jacobsen, J.K. Nørskov and M.J. Puska, Phys. Rev. B 35 (1987) 7423.
[21] O.K. Andersen, O. Jepsen and D. Glötzel, Highlights of Condensed Matter Theory LXXXIX Corso Soc. Italiana di Fisica, Bologna, 1985, p. 59.
[22] B. Hammer and J.K. Nørskov, to be published.
[23] J.A. Rodriguez and D.W. Goodman, Science 257 (1992) 897.
[24] M. Holmblad, J.H. Larsen, I. Chorkendorff, L. Pleth Nielsen, F. Besenbacher, I. Stensgaard, E. Lægsgaard, P. Kratzer, B. Hammer and J.K. Nørskov, Catal. Lett., 40 (1996) 131.
[25] J.H. Sinfelt, Bimetallic Catalysts: Discoveries, Concepts and Applications (Wiley, New York, 1983).
[26] V. Ponec, Adv. Catal. 32 (1983) 149.
[27] G. Blyholder, J. Phys. Chem. 68 (1964) 2772.
[28] P.S. Bagus and G. Pacchioni, Surf. Sci. 278 (1992) 427.
[29] R.A. Van Santen and M. Neurock, Catal. Rev., to be published.
[30] H.L. Skriver and N.M. Rosengaard, Phys. Rev. B 43 (1991) 9538.
[31] A.I. Abrikosov, H.L. Skriver, Phys. Rev. B 47 (1993) 16532.
[32] P.A. Korzhavyi, A.V. Ruban, I.A. Abrikosov and H.L. Skriver, Phys. Rev. B 51 (1995) 5773.
[33] A.I. Abrikosov, A.V. Ruban, H.L. Skriver, B. Johansson, Phys. Rev. B 50 (1994) 2039.
[34] J. Perdew and A. Zunger, Phys. Rev. B 23 (1981) 5048.
[35] D.M. Ceperley and B.J. Alder, Phys. Rev. Lett. 45 (1980) 566.
[36] K.W. Jacobsen, P. Stoltze and J.K. Nørskov, to be published.
[37] M.V. Ganduglia-Pirovano, V. Natoli, M.H. Cohen, J. Kudrnovsky and I. Turek, to be published.
[38] J.K. Nørskov, J. Chem. Phys. 90 (1989) 7461.